

PACS numbers: 42.50.Gy; 42.65.Sf; 42.65.Tg
DOI: 10.1070/QE2008v038n09ABEH013758

Polarisation effects in the formation of optical breathers at the inhomogeneously broadened $J = 0 \rightarrow J = 1$ quantum transition

A.V. Volkov, O.M. Parshkov

Abstract. **The formation and collisions of breathers excited by laser radiation at the inhomogeneously broadened $J = 0 \rightarrow J = 1$ quantum transition are studied by numerical simulations in the slowly varying envelope approximation. Conditions are obtained under which laser pulses with the initial shape quite simply realised in experiments can be transformed into elliptically polarised breathers in the medium, each of the components of their field being a breather described by the theory of self-induced transparency at a nondegenerate quantum transition. It is shown that the collision of such breathers is not elastic in the general case and leads to the appearance of more general types of resonance breather-like pulses. Taking into account relaxation processes, the possibility of the formation of a breather at the $6p^2\,{}^3P_0 \rightarrow 6p7s\,{}^3P_1$ transition in the ^{208}Pb isotope is investigated. It is found that relaxation in some case not only causes the pulse decay but also changes the eccentricity of its polarisation ellipse.**

Keywords: *breather, degenerate transition, inhomogeneous broadening, irreversible relaxation.*

1. Introduction

An optical breather, which is one of the possible pulsed structures in the self-induced transparency (SIT) theory, was first obtained as a particular solution of the sin-Gordon equation in paper [1]. The properties of a resonance breather observed in the case of SIT at a nondegenerate transition (SIT NT) were studied in detail by the method of inverse scattering problem in papers [2, 3]. The properties of breathers produced from input pulses in the case of SIT NT were also studied by this method [4 – 9].

It was shown in [10, 11] that a breather obtained in papers [1 – 3] can be considered as the limiting case of a more general double breather. In [12, 13], breathers in two-component equilibrium and nonequilibrium media were discussed outside the framework of the slowly varying envelope approximation. Nonzero optical breathers in Stark media were obtained in [14] also without using the slowly varying envelope approximation. In [12 – 14], it was assumed that the energy levels involved in quantum transitions were nondegenerate.

The consideration of the degeneracy of energy levels became a new stage in the development of the SIT theory. In particular, it was shown in [15 – 17] that the systems of SIT equations for arbitrarily polarised radiation at the $0 \leftrightarrow 1$, $1 \rightarrow 1$, and $1/2 \rightarrow 1/2$ transitions are integrable by the method of inverse scattering problem. Breather-like pulses (BLPs) at the $0 \leftrightarrow 1$ transition and arbitrarily polarised radiation were discussed in paper [18]. These pulses differ considerably from breather in the SIT NT theory in that the amplitude of their field never vanishes in the general case during finite time intervals.

Although SIT NT breathers have been theoretically discussed already for several decades, the attempts to observe them experimentally are scarce [19, 20]. In the most successful, in our opinion, experiment [20], a breather was discovered at the stage of its transformation to a decaying 0π pulse due to irreversible relaxation (see the discussion of this experiment in [21]). As far as we know, a SIT breather at degenerate quantum transitions was not observed experimentally. The main difficulty encountered in the practical realisation of a breather is the formation of a pulse of a comparatively complicated shape at the input to a resonance medium, from which a breather is then produced. The question about the properties of input radiation and distances required for the production of SIT breathers at degenerate transitions was not discussed in the literature. In addition, relaxation processes, which are very important for the practical realisation of breathers, were neglected in the papers mentioned above. This circumstance is, in our opinion, another reason for the absence of the corresponding experimental results.

The aim of this paper is to simulate numerically the formation of a breather at the $0 \rightarrow 1$ quantum transition taking into account the inhomogeneous broadening and, if necessary, relaxation processes. We described the properties of the decay of the input pulse into polarised solitons and breathers and simulated collisions of differently polarised breathers. The numerical estimates of the formation of breathers and BLPs for the $6p^2\,{}^3P_0 \rightarrow 6p7s\,{}^3P_1$ transition in the ^{208}Pb atoms are presented.

2. Formulation of the boundary-value problem

Consider a quantum transition between the lower $J = 0$ energy level and the upper $J = 1$ level, where J is the quantum number of the total angular momentum. We denote the quantum state of the nondegenerate lower level by $|1\rangle$ and the quantum states of the degenerate upper level

A.V. Volkov, O.M. Parshkov Saratov State Technical University, ul. Politekhnicheskaya 77, 410054 Saratov, Russia;
e-mail: oparshkov@mail.ru

Received 9 November 2007; revision received 18 April 2008
Kvantovaya Elektronika **38** (9) 862 – 868 (2008)
Translated by M.N. Sapozhnikov

with $M = -1, 0$ and 1 – by $|2\rangle$, $|3\rangle$, and $|4\rangle$, respectively (here, M is the quantum number of the projection of the total angular momentum on the quanitsation axis z). Let $p = (J = 0 \| \boldsymbol{p} \| J = 1)$ be the reduced matrix element of the electric-dipole moment operator for the transition under study. We assume that an ensemble of quantum objects (hereafter, called atoms) is a rarefied gas and Δ is the width (at the e^{-1} level) of the Doppler distribution density of transition frequencies ω' in atoms around the central frequency ω. Then, the polarisation decay time T_1 at the $0 \to 1$ transition due to the inhomogeneous broadening is determined by the expression $T_1 = 2/\Delta$ [22].

The electric field strength of strictly resonance radiation propagating along the z axis can be written in the form

$$\boldsymbol{E} = \mu[\boldsymbol{i}E_1 \cos(\omega t - kz + \delta_1) + \boldsymbol{j}E_2 \cos(\omega t - kz + \delta_2)]. \quad (1)$$

Here, $\mu = \sqrt{3}\hbar(T_1|p|)^{-1}$ is the normalisation factor; $\boldsymbol{i}$ and $\boldsymbol{j}$ are the unit vectors of the x and y axes, respectively; $E_{1,2}$ and $\delta_{1,2}$ are the functions of z and t describing the amplitudes and phases of oscillations of the projections of the vector $\boldsymbol{E}$ on the x and y axes, respectively; and $k = \omega/c$. It is assumed that $E_{1,2} \geqslant 0$.

Let us introduce dimensionless independent variables s and w:

$$s = z/z_0, \;\; w = (t - z/c)/T_1, \quad (2)$$

where

$$z_0 = \frac{3\hbar c}{2\pi\omega|p|^2 T_1 N};$$

N is the concentration of atoms. Let us also introduce the complex field amplitudes

$$a_1 = \frac{1}{\sqrt{2}}\left[E_1 \exp(\mathrm{i}\delta_1) - \mathrm{i}E_2 \exp(\mathrm{i}\delta_2)\right],$$

$$a_2 = \frac{1}{\sqrt{2}}\left[E_1 \exp(-\mathrm{i}\delta_1) - \mathrm{i}E_2 \exp(-\mathrm{i}\delta_2)\right].$$

Then, in the slowly varying amplitude approximation, we obtain the system of equations, which self-consistently describes the interaction of the field and medium:

$$\begin{aligned}
&\frac{\partial a_1}{\partial s} = \frac{\mathrm{i}}{\sqrt{\pi}}\int_{-\infty}^{+\infty} \sigma_{12} \exp(-\varepsilon^2)\mathrm{d}\varepsilon,\\
&\frac{\partial a_2}{\partial s} = \frac{\mathrm{i}}{\sqrt{\pi}}\int_{-\infty}^{+\infty} \sigma_{41} \exp(-\varepsilon^2)\mathrm{d}\varepsilon,\\
&\frac{\partial \sigma_{21}}{\partial w} + \mathrm{i}\varepsilon\sigma_{21} = -\mathrm{i}\left[a_1^*(\sigma_{11} - \sigma_{22}) + a_2\sigma_{24}\right] - k_1\sigma_{21},\\
&\frac{\partial \sigma_{41}}{\partial w} + \mathrm{i}\varepsilon\sigma_{41} = \mathrm{i}\left[a_2(\sigma_{11} - \sigma_{44}) + a_1^*\sigma_{42}\right] - k_1\sigma_{41},\\
&\frac{\partial \sigma_{42}}{\partial w} = \frac{\mathrm{i}}{4}(a_2\sigma_{12} + a_1\sigma_{41}),\\
&\frac{\partial \sigma_{11}}{\partial w} = \frac{1}{2}\mathrm{Im}(a_2\sigma_{14} - a_1^*\sigma_{12}) + k_2(\sigma_{22} + \sigma_{44}),\\
&\frac{\partial \sigma_{22}}{\partial w} = -\frac{1}{2}\mathrm{Im}(a_1\sigma_{21}) - k_3\sigma_{22},\\
&\frac{\partial \sigma_{44}}{\partial w} = \frac{1}{2}\mathrm{Im}(a_2^*\sigma_{41}) - k_3\sigma_{44}.
\end{aligned} \quad (3)$$

Here, σ_{ik} $(i,k = 1,2,4)$ are slowly varying amplitudes of the density matrix elements; $\varepsilon = T_1(\omega' - \omega)$; k_1, k_2, and k_3 are the rates of varying the nondiagonal and diagonal matrix elements due to spontaneous emission. Note that, due to the transverse nature of the electromagnetic field, the $|3\rangle$ state is not involved in fact in the interaction process.

We will analyse the solutions of system (3) by using the parameters a, α, and γ of the polarisation ellipse, where a is its major semiaxis measured in the units of μ and α is the angle of its inclination with respect to the x axis, and γ is the compression parameter. It is assumed usually [23] that $a \geqslant 0$, $0 \leqslant \alpha < \pi$, and $-1 \leqslant \gamma \leqslant 1$. The parameter $|\gamma|$ is the ratio of the minor and major axes of the polarisation ellipse, and the condition $\gamma > 0$ ($\gamma < 0$) corresponds to the right (left) elliptic polarisation, whereas $\gamma = 0$ corresponds to linearly polarised radiation. The parameters of the polarisation ellipse are uniquely expressed in terms of a_1 and a_2. The specification of a, α, and γ and one of the phases, for example, δ_1, uniquely determines a_1 and a_2. The corresponding cumbersome expressions are omitted here. All the parameters of the polarisation ellipse are the functions of s and w in the general case. The function $a(s,w)$ is called below the pulse envelope.

The initial conditions ($w = 0$) for system (3) are specified in the form

$$\sigma_{11} = 1, \; \sigma_{ik} = 0, \; i{\cdot}k \neq 1, \; s \geqslant 0.$$

The boundary conditions at the input to the medium ($s = 0$) have the form

$$a = a_0(w), \;\; \alpha = \alpha_0(w), \;\; \gamma = \gamma_0(w), \;\; \delta_1 = \delta_{10}(w), \;\; w \geqslant 0, \quad (4)$$

where a_0, α_0, γ_0, and δ_{10} are the specified functions of arguments s and w.

In the simplest case, function (4) has the form

$$\begin{aligned}
&\alpha_0 = \mathrm{const}, \;\; \gamma_0 = \mathrm{const},\\
&a_0(w) = |f(w;\tau,w_0) - f(w;\tau,w_0 + \Delta w)|, \;\; \delta_{10} = \Phi(w).
\end{aligned} \quad (5)$$

The function $f(w;\tau,q)$ is specified by the expression

$$f(w;\tau,q) = a_\mathrm{m}\left[\exp\left(\frac{w-q}{\tau}\right) + \exp\left(-3\frac{w-q}{\tau}\right)\right]^{-1}, \quad (6)$$

where a_m, q, and τ are parameters and the function $\Phi(w)$ is 0 for $F(w) \geqslant 0$ and π for $F(w) < 0$. Here, $F(w) = f(w;\tau,w_0) - f(w;\tau,w_0 + \Delta w)$.

The function $f(w;\tau,q)$ is described by a bell-shaped curve with the rise rate exceeding the decay rate and the FWHM equal to 1.6τ in the units of the dimensionless time w (hereafter, the time presented without indicating the time unit corresponds to the time measured in this scale). Pulses with such envelopes are commonly used in SIT experiments [24]. Expressions (4)–(6) describe a pair of 'touching' pulses obtained by the overlap of two out-of-phase elliptically polarised pulses shifted with respect to each other by the time Δw. We will call these pulses the components. Such a pair of pulses (hereafter, a composite pulse) in the case of linearly polarised laser radiation was obtained experimentally [20] and represents a 0π SIT NT pulse. A composite pulse (4)–(6) can be generated by illuminating an interference device of the type described in [20] by elliptically polarised radiation. In addition, as boundary conditions, the input pulses of a more complicated shape than (5) and (6) are used, which describe preliminarily formed optical breathers.

An important parameter of the input pulse is its area described by the expression

$$\Theta_0 = \int_{-\infty}^{+\infty} a_0(w)\sqrt{1+\gamma_0^2(w)}\,\mathrm{d}w,$$

where the integrand is proportional to the square root of the electromagnetic radiation energy flux density.

3. Analytic description of a breather

We described a breather analytically in the case of the inhomogeneously broadened $0 \to 1$ transition by using the analogy [15] between the SIT theory for such transitions and the SIT NT theory [1]. This description is also valid in the absence of irreversible relaxation and has the form

$$a = F_{\mathrm{br}}(w)\left|\frac{\cos\phi_2 - (\tau_2/\tau_1)\sin\phi_2\tanh\phi_1}{1+(\tau_2/\tau_1)^2\sin^2\phi_2\,\mathrm{sech}^2\phi_1}\right|,$$
$$\alpha = \mathrm{const},\ \gamma = \mathrm{const},\ \delta_1 = \Phi_{\mathrm{br}}(w), \tag{7}$$

where

$$F_{\mathrm{br}}(w) = \frac{4}{\tau_1\sqrt{1+\gamma^2}}\mathrm{sech}\,\phi_1;\ \phi_i = \frac{w - s/v_i + w_{0i}}{\tau_i},\ i = 1,2; \tag{8}$$

$$v_i = \sqrt{\pi}\left[\tau_1^2\int_{-\infty}^{+\infty}\frac{j_i\exp(-\varepsilon^2)\mathrm{d}\varepsilon}{(\tau_1/\tau_2 - \varepsilon\tau_1)^2+1}\right]^{-1},$$
$$j_1 = 1,\quad j_2 = \varepsilon\tau_2 - 1. \tag{9}$$

Here, $\Phi_{\mathrm{br}}(w)$ is the function taking values 0 or π for the negative or nonnegative values of the quantity in the modulus in (7), respectively. We will call the function $F_{\mathrm{br}}(w)$ the secondary envelope breather. The quantity v_1 is the group velocity of the breather equal to the propagation velocity of its secondary envelope. The important parameters determining the breather structure are τ_1 ($\tau_1 > 0$), τ_2 ($-\infty < \tau_2 < \infty$), and γ. The constant α depends on the orientation of the x and y axes, while constants w_{01} and w_{02} are determined by the choice of the reference point of the coordinate s and time w. Note that the components of the breather field (7)–(9) along the x and y axes have the form of SIT NT breathers shifted in phase with respect to each other.

Expressions (7)–(9) are used below to find breathers in calculation results (see section 4.1) and to specify the radiation envelope describing a breather at the input to a resonance medium (see section 4.2).

As mentioned above, it was shown in [18] that SIT at the $0 \to 1$ quantum transition admits solutions describing BLPs. Breather-like pulses are characterised by four independent parameters. A breather described by expressions (7)–(9) should be a particular case of such BLPs. However, the inhomogeneous broadening was neglected in [18] and the BLP velocity in the presence of the inhomogeneous broadening was not obtained.

4. Results of calculations

4.1 Breather formation process

Consider the formation of a breather by neglecting relaxation processes. Let us assume in (5) and (6) that $a_{\mathrm{m}} = 0.25$, $\tau = 14$, $\Delta w = 22$, and $w_0 = 40$, so that $\Theta_0 = 1.8\pi$. In this case, the duration of each component pulse is equal to the time shift between pulses and considerably exceeds the time T_1. In this case, we are dealing with the large inhomogeneous broadening. We also assume that $\alpha_0 = \pi/6$, and $\gamma_0 = 0.5$. The pulse envelopes for $s = 0$ and 6 are shown in Fig. 1 (the values of α and γ for any s are equal to $\pi/6$ and 0.5, respectively). Let us show that Fig. 1b presents the breather envelope.

The height of the central peak of the pulse in Fig. 1b is 0.0659. Let us assume that it coincides with the coefficient at $\mathrm{sech}\,\phi_1$ in the first expression in (8). Then, taking into account that $\gamma = 0.5$, we obtain $\tau_1 = 54.26$. By using again the first expression in (8), we can construct the dependence of the secondary envelope $F_{\mathrm{br}}(w)$ with an accuracy to the position on the w axis. This dependence is shown in Fig. 1b by the dotted curve with the maximum made coincident with the maximum of the central peak. Good coincidence of the dotted curve with the pulse envelope suggests that Fig. 1b demonstrates a breather. The parameter τ_2 can be estimated from the expression $\tau_2 = x_{\mathrm{m}}\tau_1$, where x_{m} is the maximal root of the equation

$$\cos(\xi/x) - x\sin(\xi/x)\tan\xi = 0.$$

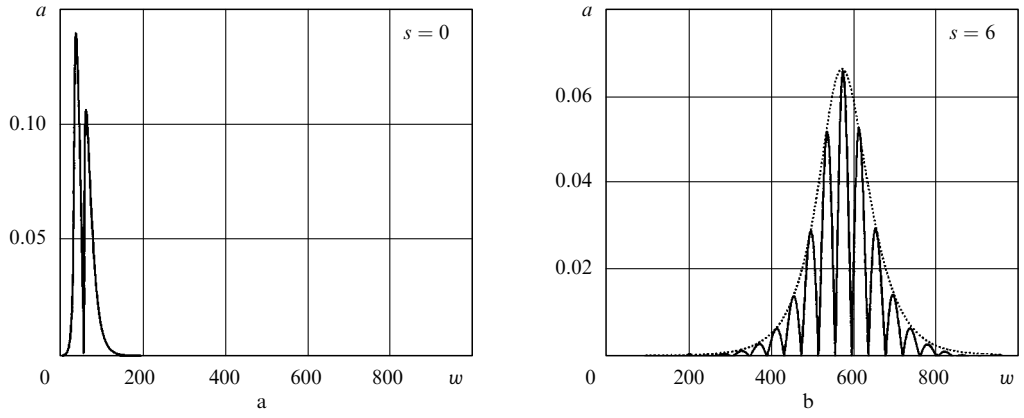

Figure 1. Envelopes of the input pulse (a) and breather at a distance of $s = 6$ (b). The dotted curve is the secondary envelope of the breather.

Here, $\xi = \Delta\tau/\tau_1$; and $\Delta\tau$ is the half-width of the base of the central peak of the breather. We find by this method the value of $\tau_2 = 13.46$ and, by using expression (9), obtain $v_1 = 1.067 \times 10^{-2}$. According to the calculation results presented in Fig. 1b, we have $v_1 = 1.070 \times 10^{-2}$. The close values of the group velocity v_1 obtained by these two methods confirms the fact that Fig. 1b demonstrate a breather.

Calculations performed for different combinations of quantities a_m, τ ($\tau \geqslant 1$), and Δw in expressions (5) and (6) under the condition that $|\Delta w - 1.6\tau|/\tau < 0.5$ well agree with the statement that the radiation structure at long distances is determined by the interval $\Delta_l \equiv (\bar{\Theta}_{l-1}, \bar{\Theta}_l)$ ($l = 1, 2, 3, ...$) where the input pulse area Θ_0 is located. The numbers $\bar{\Theta}_l$ are specified by expressions

$$\bar{\Theta}_l = (4[l/2] + 3\{l/2\})\pi, \tag{10}$$

where $[a]$ and $\{a\}$ are the integer and fractional parts of the number a. For $\Theta_0 < 1.5\pi$, i.e. when Θ_0 is located in the first interval $\Delta_1 = (\bar{\Theta}_0, \bar{\Theta}_1)$, a pulse consisting of many peaks is formed, which decays with distance. If $\Theta_0 > 1.5\pi$ and belongs to an interval with an odd number Δ_l, only l pairs of 2π pulses are formed in the medium; if the interval has an even number, a breather appears along with 2π pulses.

In the case of calculations presented in Fig. 1, the area Θ_0 is located in the second interval, for which $[\Theta_0/(4\pi)] = 0$, so that only a breather should be formed, which is confirmed by calculations. Figure 2 presents the results obtained for $a_m = 1.48$ and the same other conditions as in the previous calculation. In this case, $\Theta_0 = 10.5\pi$ and is located in the sixth interval, for which $[\Theta_0/(4\pi)] = 2$, so that two pairs of 2π pulses and one breather should appear. This assumption is confirmed by Fig. 2.

Our calculations showed that for Θ_0 slightly exceeding 1.5π, the breather duration considerably exceeds the input pulse duration and the breather consists of many well resolved peaks. For Θ_0 slightly smaller than 4π, the breather duration is small and it consists of a small number of subpulses. The role of intervals Δ_l for circularly polarised pulses was discussed in detail in paper [25], and therefore we will restrict ourselves by the examples considered above.

4.2 Collision of pulses

Consider two breathers (7) – (9) arriving successively at the input ($s = 0$) of a medium. The parameters for the first breather [(*1*) in Fig. 3a] are $\tau_1 = 54$, $\tau_2 = 13$, $w_{01} = 300$, and $w_{02} = 20$ and for the second breather [(*2*) in Fig. 3a] $\tau_1 = 11$, $\tau_2 = 19$, $w_{01} = 1000$, and $w_{02} = 20$. Both breathers are linearly polarised at an angle of 45° to each other. Figure 3b presents the envelopes of these breathers before their collision and Fig. 3c illustrates the overlap of these pulses. Note that after the collision (Fig. 3d), pulses (*1*) and (*2*) are no longer breathers because the field nowhere vanishes within these pulses. Therefore, these pulses can be assigned to BLPs described in paper [18]. Breather-like pulses propagate in a medium like breathers, periodically changing their shape without loosing energy. At least calculations performed for $s = 14 - 20$ did not reveal any energy losses, although the field strength of weak monochromatic radiation should decrease at such distance due to the inhomogeneous broadening approximately by 4×10^3 times [22].

Breather-like pulses are linearly polarised, their polarisation planes rotating in the opposite directions: counterclockwise for pulse (*1*) and clockwise for pulse (*2*) when looking toward the wave. This circumstance is illustrated in Fig. 4 presenting the fragments of Fig. 3d containing the envelopes of pulses (*2*) and (*1*) together with functions $\alpha(w)$. Recall that SIT NT breathers recover their shape after a collision [26]. Our calculations showed that breathers linearly polarised at an angle of 90° to each other have such properties (these properties are obvious for the zero angle, because the corresponding problem is the SIT NT problem).

The experimental realisation of input pulses in the form of breathers (7) – (9) is complicated. Because of this, we will assume that two composite pulses [(*1*) and (*2*) in Fig. 5a] arrive successively at the input surface $s = 0$. We assume that $a_m = 0.25$, $w_0 = 40$, $\alpha = 0$, and $\Theta_0 = 1.8\pi$ for pulse (*1*) and $a_m = 0.42$, $w_0 = 700$, $\alpha = \pi/4$, and $\Theta_0 = 3\pi$ for pulse (*2*). Pulse (*1*) has the left elliptic polarisation and pulse (*2*) has the right elliptic polarisation, and $|\gamma| = 0.5$ for both pulses. Pulse (*1*) is transformed in the medium to a breather [(*1*) in Fig. 5b] with $\tau_1 = 54.26$, $\tau_2 = 13.67$, $\alpha = 0$, and $\gamma = -0.5$. Input pulse (*2*) produces a BLP [(*2*) in Fig. 5b]. Pulse (*2*) is transformed to the BLP instead of a breather because this pulse interacts at the initial formation stage with the medium coherently excited by pulse (*1*). Note that the medium remains in the unexcited state after the breather. This circumstance was favourable for the formation of breather (*2*) in Fig. 3b. After a collision, each pulse has the BLP structure, which is similar to that shown in Fig. 3c.

4.3 Influence of relaxation

We perform numerical estimates for the 283.3-nm $6p^2\,{}^3P_0 \rightarrow 6p7s\,{}^3P_1$ transition in the ^{208}Pb isotope in saturated vapour at temperatures 900 – 1100 K. This transition was used in experimental studies of electromagnetically induced transparency [27]. By using the oscillator strengths taken from [28], we find $|p|^2 =$

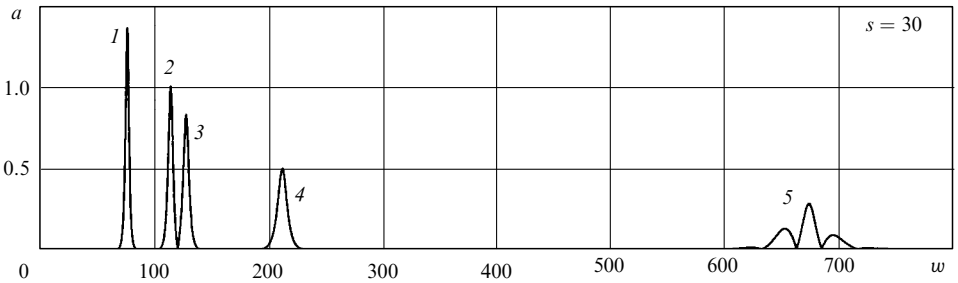

Figure 2. Decay of the input pulse with the area $\Theta_0 = 10.5\pi$: 2π pulses (*1–4*) and a breather (*5*).

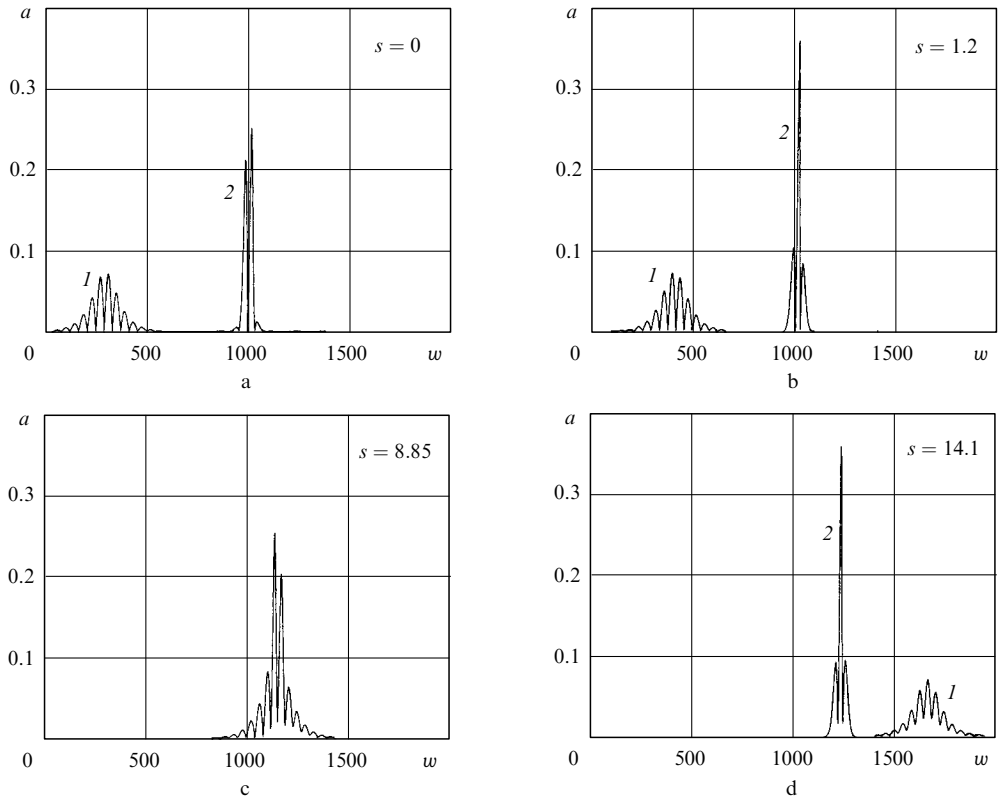

Figure 3. Collision of linearly polarised breathers: breathers at the input to a resonance medium (a), isolated breathers before the collision (b), the overlap of breathers (c), BLPs after the collision.

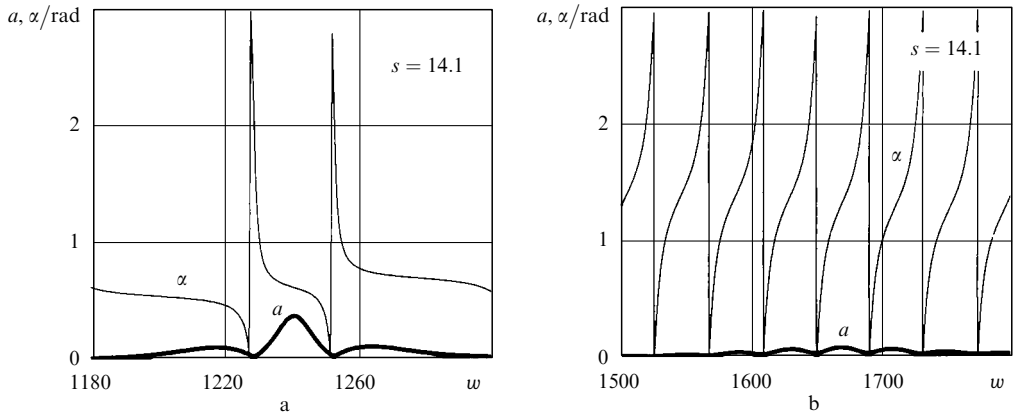

Figure 4. Fragments of Fig. 3d containing BLP (*2*) (a) and BLP (*1*) (b), and functions $\alpha(w)$.

1.2×10^{-35} CGSE units. For $T = 1000$ K, we have $T_1 = 1.6 \times 10^{-10}$ s and $N = 1.1 \times 10^{14}$ cm^{-3} [29], so that $z_0 = 0.011$ cm. Relaxation at low pressures is caused by the spontaneous decay of the upper $6p7s\,^3P_1$ level to the $6p^2\,^3P_i$ ($i = 0,\ 1,\ 2$) levels. By using data [28], we obtain $k_1 = 1.4 \times 10^{-2}$, $k_2 = 8.8 \times 10^{-3}$, and $k_3 = 2.9 \times 10^{-2}$. The FWHM $\tau_{1/2}$ (in seconds) of component pulse (6) is $2.5 \times 10^{-10}\tau$ and its peak intensity (in W cm^{-2}) is $I_m = 424a_m^2(1 + \gamma^2)$. A change in temperature within 900–1100 K affects considerably only the values of N and z_0. Thus, $z_0 = 0.11$ and 0.0016 cm for $T = 900$ K and 1100 K, respectively.

Figure 6a presents the results of calculations for the same boundary conditions as in Fig. 1. This means that $\tau_{1/2} = 3.5$ ns and $I_m = 33$ W cm^{-2}. Instead of the breather (see Fig. 1b), a pulse appears now, which rapidly decays during propagation. The envelopes of this pulse for $s = 2$ and 3 are presented in Fig. 6a. The rapid decay of the pulse is explained by the following reason. For this calculation, $\Theta_0 = 1.8\pi$ and the breather duration is $\sim$400 (see Fig. 1b), which is approximately four times longer than the duration of the input composite pulse. The shortest of the relaxation times is $1/k_1 = 71$. Therefore, coherent processes lead to such an increase in the pulse duration in the medium that it becomes considerably longer then the irreversible relaxation times. Under these conditions, relaxation efficiently suppresses the breather.

The situation when $a_m = 0.523$ and all other conditions coincide with the conditions of the previous calculation is illustrated in Fig. 6b. Then, $\Theta_0 = 3.7\pi$, $\tau_{1/2} = 3.5$ ns, and $I_m = 145$ W cm^{-2}. This figure presents the envelopes of pulses for $s = 2.8$ and 4 and also the envelope of a breather

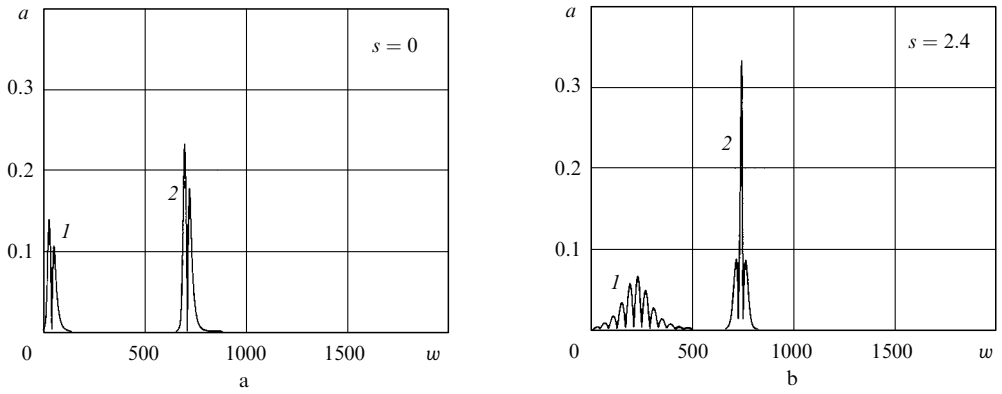

Figure 5. Appearance of an elliptically polarised breather and a BLP: composite pulses (*1*) and (*2*) at the input to a medium (a), breather (*1*) and BLP (*2*) inside the medium (b).

that could appear in the absence of relaxation. One can see that the breather is also quite efficiently suppressed by relaxation in this case. However, the pulse envelope at the distance $s = 2.8$ (about 3 mm for $T = 900$ K) looks like the breather envelop. The matter is that, as mentioned above, for $\Theta_0 = 3.7\pi$ the breather has a comparatively short duration. In particular, the intensity of breather (*3*) in Fig. 6b is smaller more than by half than that of the breather in Fig. 1b. Therefore, relaxation weakly affects the pulse formation process and the pulse can resemble a breather at small distances. The numerical analysis performed in [21] showed that such a pulse resembling a breather was observed in experiments [20] in the case of linearly polarised radiation.

Relaxation affects not only the evolution of the major axis of the polarisation ellipse but also the compression parameter γ. This is illustrated by Fig. 7 showing the envelope of pulse (*1*) presented in Fig. 6b together with the dependence of γ on w. It follows from Fig. 7 that relaxation not only changes considerably $|\gamma|$ but also its sign. This means that the rotation direction of the vector $\boldsymbol{E}$ changes. Relaxation does not affect the angle α, and this angle is equal to $\pi/6$ at all distances, as for the input pulse.

Figure 8 shows the results of calculations for $\tau = 0.2$, $a_m = 35.77$, and the same parameters of the boundary conditions as in Fig. 1 (for this value of τ, the inhomogeneous broadening should be considered small). In the given case, $\Theta_0 = 3.7\pi$, $\tau_{1/2} = 50$ ps, and $I_m = 68$ kW cm^{-2}. The

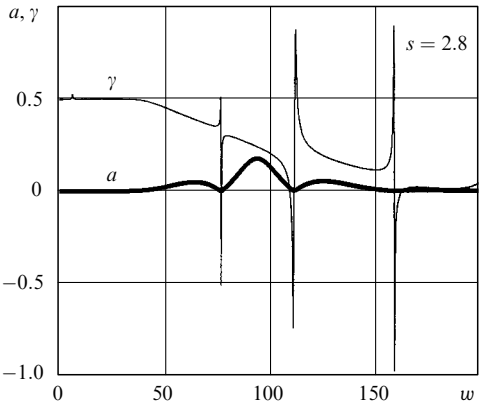

Figure 7. Fragment of Fig. 6b containing the envelope of pulse (*1*), and the dependence $\gamma(w)$.

solid curves in Fig. 8 show the envelopes of pulses for $s = 256$ and 283 taking relaxation into account, and the dotted curves show the envelopes of breathers for $s = 283$ and 318 in the absence of relaxation. For $T = 1000$ K, the smallest and greatest of these distances are 2.8 and 3.5 cm, respectively (distances were selected so that the solid and dotted curves had similar shapes). In all calculations for any s and w, we obtained $\alpha = \pi/6$ and $\gamma = 0.5$, as for the input pulse. Note that each pulse structure in Fig. 8 contains a prepulse consisting of many peaks and a tail, which decay

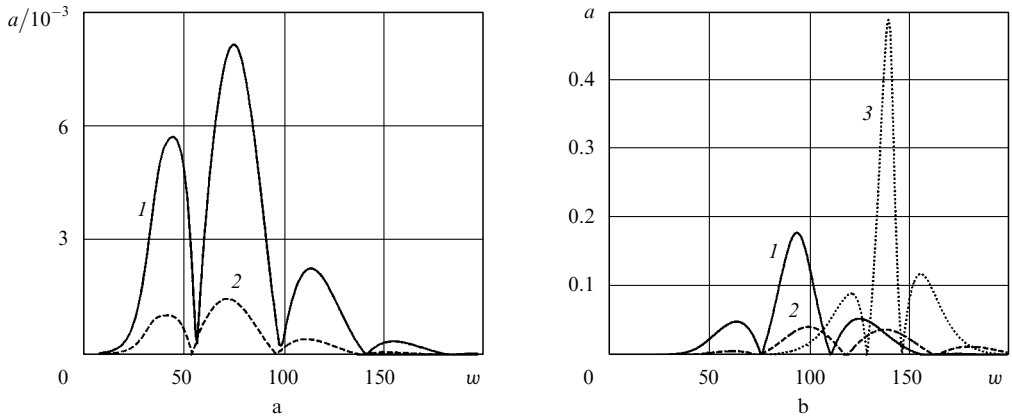

Figure 6. Pulses in the presence of relaxation for $s = 2$ (*1*) and 3 (*2*) for $\Theta_0 = 1.8\pi$ (a) and pulses in the presence of relaxation for $s = 2.8$ (*1*) and 4 (*2*), and a breather in the absence of relaxation for $s = 7.86$ (*3*) for $\Theta_0 = 3.7\pi$ (b).

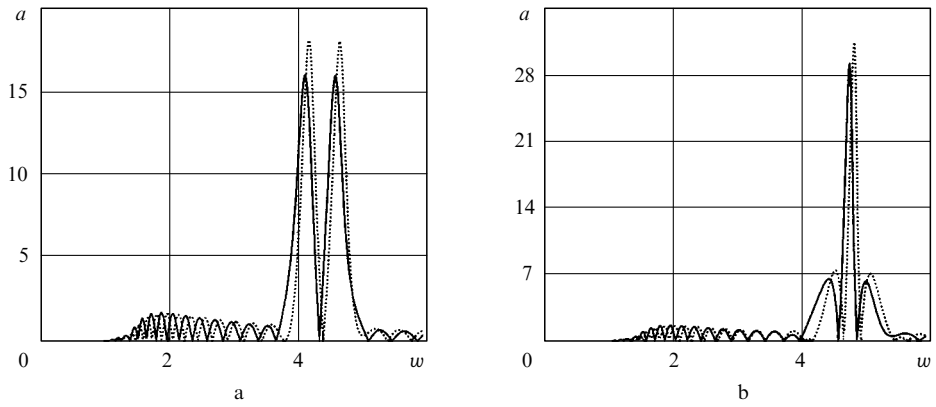

Figure 8. Pulses in the presence of relaxation (solid curves) and breathers in the absence of relaxation (dotted curves) for $\Theta_0 = 3.7\pi$ and small durations of input pulses: a pulse for $s = 256$ and a breather for $s = 283$ (a), a pulse for $s = 283$ and a breather for $s = 318$ (b).

during the pulse propagation even in the absence of relaxation.

The close shapes of the solid and dotted curves demonstrate a weak influence of relaxation on the development of the process. This is explained by a short duration of the input pulse and the closeness of the value of Θ_0 to 4π. These conditions provide the appearance of a breather of duration 1 (see the dotted curves in Fig. 8), which is considerably smaller than the smallest of the relaxation times $1/k_1 = 71$. Note that in this case, relaxation leads to a small decrease in the pulse velocity (approximately by 10 %) and almost the same decrease in the spatial period of the reconstruction of the shape of its envelope.

5. Conclusions

Our calculations have revealed the following features related to the influence of the polarisation of input laser radiation on the breather formation process. First, we have shown that an elliptically polarised composite pulse with fixed values of α and γ incident on a medium can produce a breather with the same values of α and γ. The numerical analysis performed in the paper gives a simple rule relating the structure of radiation at large distances with the area of the composite pulse. This rule generalises the rule proposed in [24] for the cases of circularly and linearly polarised radiation.

Second, the collision of breathers is followed by the recovery of their initial shape only in some particular cases (for example, for circular polarisations, collinear or orthogonal linear polarisations). In the general case, this collision will result in the formation of two BLPs with parameters of the polarisation ellipse depending on the time and coordinate in a complicated way. When two elliptically polarised composite pulses arrive successively at the input of a resonance medium, only the first of them produces a breather, whereas the second pulse is transformed to a BLP. This is explained by the influence of the coherent excitation of the medium remained after the propagation of the first pulse. The collision of the elliptically polarised breather and BLP gives rise in the general case to two BLPs.

Under typical conditions of a possible experiment, relaxation prevents the formation of a breather from the input composite nanosecond pulses. Relaxation affects not only the pulse envelope but also the compression parameter of the polarisation ellipse. For input composite pulses of duration ~ 100 ps, the influence of relaxation is negligible, at least when Θ_0 is only slightly smaller than 4π.

References

1. Lamb G.L. Jr. *Rev. Mod. Phys.*, **43**, 99 (1971).
2. Ablovitz M.J., Kaup D.J., Newell A.C. *J. Math. Phys.*, **15**, 1852 (1974).
3. Lamb G.L. Jr. *Phys. Rev. A*, **9**, 422 (1974).
4. Hopf F.A., Shakir S. *Phys. Rev. A*, **19**, 243 (1979).
5. Shakir S.A. *Phys. Rev. A*, **20**, 1579 (1979).
6. Shakir S.A. *Opt. Commun.*, **33**, 99 (1980).
7. Kaup D.J., Scacca L.R. *J. Opt. Soc. Am.*, **70**, 224 (1980).
8. Andreev V.A. *Kvantovaya Elektron.*, **10**, 2045 (1983) [*Sov. J. Quantum Electron.*, **13**, 1364 (1983)].
9. Manykin E.A., Zakharov S.M., Onishchenko E.V. *Zh. Eksp. Teor. Fiz.*, **105**, 1583 (1994).
10. Adamashvili G.T. *Opt. Spektrosk.*, **85**, 95 (1998).
11. Adamashvili G.T., Adamashvili N.T., Koplatadze R.R., Motsonelidze G.N., Peikrishvili M.D. *Opt. Spektrosk.*, **96**, 864 (2004).
12. Sazonov S.V. *Zh. Eksp. Teor. Fiz.*, **119**, 419 (2001).
13. Sazonov S.V. *Usp. Fiz. Nauk*, **171**, 663 (2001).
14. Elyutin S.O. *Zh. Eksp. Teor. Fiz.*, **128**, 17 (2005).
15. Basharov A.M., Maimistov A.I. *Zh. Eksp. Teor. Fiz.*, **87**, 1594 (1984).
16. Chernyak V.Ya., Rupasov V.I. *Phys. Lett. A*, **108**, 434 (1985).
17. Basharov A.M., Maimistov A.I., Sklyarov Yu.M. *Opt. Spektriosk.*, **63**, 707 (1987).
18. Steudel H. *J. Mod. Opt.*, **35**, 693 (1988).
19. Hamadani S.M., Goldhar J., Kurnit N.A., Javan A. *Appl. Phys. Lett.*, **25**, 160 (1974).
20. Diels J.C., Hahn E.L. *Phys. Rev. A*, **10**, 2501 (1974).
21. Parshkov O.M. *Kvantovaya Elektron.*, **37**, 813 (2007) [*Quantum Electron.*, **37**, 813 (2007)].
22. Akulin V.M., Karlov N.V. *Intensivnye rezonansnye vzaimodeistviya v kvantovoi elektronike* (Intense Resonance Interactions in Quantum Electronics) (Moscow: Nauka, 1987).
23. Born M., Wolf E. *Principles of Optics* (Oxford: Pergamon Press, 1969; Moscow: Nauka, 1973).
24. Slusher R.E., Gibbs H.M. *Phys. Rev. A*, **5**, 1634 (1972).
25. Dmitriev A.E., Parshkov O.M. *Kvantovaya Elektron.*, **34**, 652 (2004) [*Quantum Electron.*, **34**, 652 (2004)].
26. Dodd R.K., Eilbeck J.C., Gibbon J., Morris H.C. *Solitons and Nonlinear Wave Equations* (New York: Academic Press, 1982; Moscow: Mir, 1988).
27. Kasapi A., Maneesh Jain, Yin G.Y., Harris S.E. *Phys. Rev. Lett.*, **74**, 2447 (1995).
28. DeZafra R.L., Marshall A. *Phys. Rev.*, **170**, 28 (1968).
29. Grigor'ev I.S., Meilikhov E.Z. (Eds) *Fizicheskie velichiny. Spravochnik* (Handbook of Physical Quantities) (Moscow: Energoatomizdat, 1991).